PHYSICAL REVIEW D **84,** 085006 (2011)

Extremely high energy neutrinos from cosmic strings

Veniamin Berezinsky,[1,*] Eray Sabancilar,[2,†] and Alexander Vilenkin[2,‡]

[1]*INFN, Laboratori Nazionali del Gran Sasso, I–67010 Assergi (AQ), Italy*

[2]*Institute of Cosmology, Department of Physics and Astronomy, Tufts University, Medford, Massachusetts 02155, USA*

(Received 11 August 2011; published 11 October 2011)

Superstring theory and other supersymmetric theories predict the existence of relatively light, weakly interacting scalar particles, called moduli, with a universal form of coupling to matter. Such particles can be emitted from cusps of cosmic strings, where extremely large Lorentz factors are achieved momentarily. Highly boosted modulus bursts emanating from cusps subsequently decay into gluons; they generate parton cascades which in turn produce large numbers of pions and then neutrinos. Because of very large Lorentz factors, extremely high energy neutrinos, up to the Planck scale and above, are produced. For some model parameters, the predicted flux of neutrinos with energies $\gtrsim 10^{21}$ eV is observable by JEM-EUSO and by the future large radio detectors LOFAR and SKA.

DOI: 10.1103/PhysRevD.84.085006 PACS numbers: 11.27.+d, 98.70.Sa, 98.80.Cq

I. INTRODUCTION

Cosmic strings could be formed as topological defects in the early universe. They are predicted in a wide class of particle physics models and can produce a variety of observational effects. These include gravitational lensing, linear discontinuities in the cosmic microwave background, and gravitational radiation, both in the form of a stochastic background and localized bursts. (For a review of cosmic strings, see, e.g., [1,2].)

Strings predicted in many grand unified models respond to external electromagnetic fields as thin superconducting wires [3]. As they move through cosmic magnetic fields, such strings develop electric currents. Oscillating loops of current-carrying string emit highly boosted charged particles from cusps—short segments where the string velocity momentarily gets very close to the speed of light. The emitted particles and their decay products can then be observed as high-energy cosmic rays [4] and gamma-ray bursts [5–7].

A phenomenon closely related to string superconductivity is the development of a bosonic condensate around the string core [3]. For example, a condensate of standard model Higgs particles could form around strings in some models. The Higgses would then be copiously produced at cusps, and their decay products could reach the Earth as cosmic rays [8].

Here we shall discuss an alternative mechanism of cosmic ray production, which does not assume string superconductivity or Higgs condensates. It relies on the existence of moduli—relatively light, weakly coupled scalar fields, predicted in supersymmetric particle theories, including string theory. Moduli would be copiously radiated by oscillating loops of string at early cosmic times, when the loops are smaller than the modulus Compton wavelength, $L < 1/m$, and their frequency of oscillation is greater than the modulus mass. The emitted moduli may affect the big bang nucleosynthesis as they decay into photons and baryons, and contribute to dark matter and to diffuse gamma-ray background, resulting in stringent constraints on both the cosmic string tension and the modulus mass, when moduli are assumed to have gravitational-strength couplings to matter [9–12]. However, the couplings may in fact be much stronger, in which case the constraints from moduli radiation may be significantly relaxed [12]. Such strongly coupled moduli appear to be quite generic in string theory landscape [13–18], and this case is of particular interest for production of extremely high energy (EHE) cosmic rays and neutrinos.

At later times, moduli can only be emitted from cusps, resulting in sharp bursts of high-energy moduli. Eventually moduli decay into standard model particles, and their decay products can be observed as cosmic rays with energies above 10^{21} eV.

The great interest of cosmic strings, and more generically topological defects, in high-energy neutrino astronomy is based on tremendous energies of neutrinos accessible for these sources. While astrophysical sources can accelerate particles to energies 10^{21}–10^{22} eV at most, topological defects can produce particles, including neutrinos, up to the Planck scale and above. Many observational methods of neutrino detection, in particular, radio observations and observation of fluorescent light from space, are possible only above $\sim 10^{20}$ eV. Detection of such high-energy neutrinos can by itself be considered as a signature of neutrinos from topological defects or other top-down scenarios. The production of EHE particles is a very generic property of topological defects, cosmic strings, in particular, but large fluxes of such particles are produced only in exceptional cases [4,19–22].

In this paper, we shall treat the modulus mass and coupling constant and the string tension as free parameters.

*venya.berezinsky@lngs.infn.it
†eray.sabancilar@tufts.edu
‡vilenkin@cosmos.phy.tufts.edu

 © 2011 American Physical Society

We shall estimate the EHE neutrino flux resulting from modulus decays and indicate some values of the parameters that can yield observable fluxes. The paper is organized as follows. In Sec. II, we review modulus emission from cosmic string cusps (a more detailed derivation is given in the Appendix). In Sec. III, we discuss modulus decay, EHE neutrino production, including beaming, and propagation in the universe. In Sec. IV, we review the size distribution of cosmic string loops and calculate the rate of bursts and the diffuse flux of EHE neutrinos. We also discuss here the upper bound on the neutrino flux, resulting from the diffuse gamma-ray background observations. At the end of that section we give two illustrative examples of neutrino fluxes for different values of the model parameters. Finally, we discuss EHE neutrino detection. Conclusions are presented in Sec. V.

II. MODULUS RADIATION FROM STRINGS

The effective action for a modulus field ϕ interacting with a cosmic string of tension μ is given by [9]

$$S = -\int d^4x\left[\frac{1}{2}(\nabla\phi)^2 + \frac{1}{2}m^2\phi^2 + \frac{\sqrt{4\pi}\alpha}{m_p}\phi T^\nu_\nu\right] - \mu\int d^2\sigma\sqrt{-\gamma}, \quad (1)$$

where γ is the determinant of the induced world sheet metric $\gamma_{ab} = g_{\mu\nu}X^\mu_{,a}X^\nu_{,b}$, $X^\mu(\sigma,\tau)$ is the string world sheet, T^ν_ν is the trace of the energy momentum tensor of the string, α is the modulus coupling constant, m is the modulus mass, and m_p is the Planck mass. For $\alpha \sim 1$, the modulus coupling to matter is suppressed by the Planck scale. Here, we treat α as a free parameter and are mainly interested in $\alpha \gg 1$. Then, the mass scale characterizing the modulus interactions is $\sim m_p/\alpha \ll m_p$. Values as large as $\alpha \sim 10^{15}$ have been discussed in the literature [17].

The modulus field equation has the form

$$(\nabla^2 - m^2)\phi(x) = -\frac{\sqrt{4\pi}\alpha}{m_p}T^\nu_\nu(x), \quad (2)$$

with

$$T^\nu_\nu(x) = -2\mu\int d\tau d\sigma\sqrt{-\gamma}\delta^4(x^\alpha - X^\alpha(\sigma,\tau)). \quad (3)$$

The power spectrum of modulus radiation from an oscillating loop of string can be decomposed in Fourier modes as [9]

$$\frac{dP_n}{d\Omega} = \frac{G\alpha^2}{2\pi}\omega_n k|T(\mathbf{k},\omega_n)|^2, \quad (4)$$

where G is the Newton's constant, $\omega_n = \sqrt{k^2+m^2} = 4\pi n/L$, L is the length of the loop,

$$T(\mathbf{k},\omega_n) = -\frac{4\mu}{L}\int d^4x \times \int d\sigma d\tau\sqrt{-\gamma}\delta^4(x^\alpha - X^\alpha(\sigma,\tau))e^{ik_\nu X^\nu(\sigma,\tau)}, \quad (5)$$

and $k^\nu = (\omega_n, \mathbf{k})$.

We shall be interested in the modulus emission from large loops of string, having length $L \gg m^{-1}$. In this case, the characteristic frequency of loop oscillation is $\omega \sim 1/L \ll m$, so modulus production is suppressed, except in the vicinity of cusps, where extremely high frequencies can be reached in a localized portion of the loop for a brief period of time. Lorentz factors greater than[1] γ are reached in a fraction of the loop of invariant length $\Delta L \sim L/\gamma$.

The spectrum of resulting particle bursts can be found by expanding $X^\mu(\sigma,\tau)$ near a cusp [8,10].[2] One finds that the number of moduli emitted in a single burst with momenta k in the interval dk (in the center of mass frame of the loop) is given by

$$dN(k) \sim \alpha^2 G\mu^2 L^{2/3}k^{-7/3}dk. \quad (6)$$

This distribution applies for $k > k_c$, where

$$k_c \sim \frac{1}{4}m\sqrt{mL}. \quad (7)$$

At smaller k the distribution is strongly suppressed, $dN \approx 0$.

The dominant contribution to the modulus emission comes from the lower momentum cutoff $k_{\min} \sim k_c$, so the total number of moduli per burst is

$$N \sim \frac{\alpha^2 G\mu^2}{m^2}. \quad (8)$$

The particles come from a portion of the loop that reaches Lorentz factors in excess of

$$\gamma_c \sim k_c/m \sim \frac{1}{4}\sqrt{mL}, \quad (9)$$

and are emitted into a narrow opening angle ϑ_c around the direction of the string velocity $\mathbf{v}$ at the cusp,

$$\vartheta_c \sim \gamma_c^{-1} \sim 4(mL)^{-1/2}. \quad (10)$$

The total power of modulus radiation can be similarly calculated as

$$P_m \sim \alpha^2 G\mu^2 L^{-1/3}k_c^{-1/3} \sim \frac{\alpha^2 G\mu^2}{\sqrt{mL}}. \quad (11)$$

[1] From here on, and until Appendix, we use the notation γ only for the Lorentz factor.

[2] A detailed analysis of particle emission from cusps is given in the Appendix, confirming the results obtained in [8,10].

The loops also radiate gravitational waves with the power

$$P_g \sim \Gamma G\mu^2, \tag{12}$$

where $\Gamma \approx 50$ [1]. $P_g \sim P_m$ when $L \sim L_*$ which is given by

$$L_* \sim \Gamma^{-2}\alpha^4 m^{-1}. \tag{13}$$

The lifetime of a loop which mainly radiates gravitationally is

$$\tau_g \sim \frac{\mu L}{P_g} \sim \frac{L}{\Gamma G\mu}, \tag{14}$$

which implies that the characteristic size of the smallest (and most numerous) loops surviving at time t is

$$L^g_{\min} \sim \Gamma G\mu t. \tag{15}$$

On the other hand, modulus radiation dominates when $P_g \lesssim P_m$ and the loop lifetime is given by

$$\tau_m \sim \frac{\mu L}{P_m} \sim \frac{L^{3/2}m^{1/2}}{\alpha^2 G\mu}. \tag{16}$$

The corresponding minimum loop size at time t is

$$L^m_{\min} \sim \alpha^{4/3}(G\mu)^{2/3}m^{-1/3}t^{2/3}. \tag{17}$$

The transition between the two regimes occurs at

$$t_* \sim \frac{\alpha^4}{\Gamma^3 G\mu m}. \tag{18}$$

Therefore, the minimum loop length is given by (15) for $t \gtrsim t_*$ and by (17) for $t \lesssim t_*$. The redshift corresponding to t_* is given by

$$z_* \sim \Gamma^2\alpha^{-8/3}(G\mu)^{2/3}(mt_0)^{2/3}, \tag{19}$$

numerically

$$z_* \sim 400 m_5^{2/3}\alpha_7^{-8/3}\mu_{-20}^{2/3}, \tag{20}$$

where

$$m_5 = m/10^5\,\text{GeV}, \quad \alpha_7 = \alpha/10^7, \quad \mu_{-20} = G\mu/10^{-20}, \tag{21}$$

and the fiducial values have been chosen anticipating the results in Sec. IV.

III. NEUTRINO PRODUCTION AND PROPAGATION

In this section we address some problems in neutrino physics relevant for future consideration, namely, the neutrino horizon, the energy spectrum of neutrinos produced by a modulus decay, the boost of this spectrum by the cusp Lorentz factor, and some others.

We start with a note about accuracy of our calculations. The main purpose of our work is a discussion of the principle features of the phenomenon, i.e., EHE neutrino production by moduli from cosmic strings, not an accurate numerical evaluation of the neutrino fluxes and their detection rates. In particular, our aim is to express the results in the form of analytical formulas, so that the dependence on input parameters can be easily seen. For this purpose we make the following simplifying assumptions.

We use the cold dark matter cosmological model with $\Lambda = 0$ and $\Omega_m + \Omega_r = 1$ and use $H_0 = 72$ km/s Mpc, $t_0 = 4.3 \times 10^{17}$ s, $t_{\rm eq} = 2.4 \times 10^{12}$ s, $1 + z_{\rm eq} = 3200$, the scale factor in the radiation- and matter-dominated eras are $a_r(t) \propto t^{1/2}$ and $a_m(t) \propto t^{2/3}$. The corresponding time-redshift relations are, respectively, given by $(t/t_0) = (1 + z_{\rm eq})^{1/2}(1 + z)^{-2}$ and $(t/t_0) = (1 + z)^{-(3/2)}$.

For convenience of calculations we assume that at the decay of a modulus at rest the neutrino spectrum is $\propto E^{-2}$, while in reality this spectrum is not power law and is approximately proportional to $E^{-1.9}$ only for a very large mass of the decaying particle.

A. Neutrino horizon

As they propagate through the universe, the ultrahigh-energy (UHE) neutrinos ν_i (or antineutrino $\bar\nu_i$) with $i = e$, μ, τ are absorbed or lose energy in the following three reactions [23]:

$$(i)\ \bar\nu_i + \nu_i \to q_\alpha + \bar q_\alpha, \qquad (ii)\ \nu_i + \bar\nu_i \to l + \bar l,$$
$$(iii)\ \nu_i + \bar\nu_j \to \nu_i + \bar\nu_j, \tag{22}$$

where $q = u_\alpha, d_\alpha, s_\alpha, c_\alpha, b_\alpha$ are quarks with $\alpha = 1, 2, 3$ being color indices and $l = e$, μ, τ are lepton flavors. Reactions (i) include only s channel and (ii) may include both s and t channels. For a rough estimate we can use the following approximation for the cross section,

$$\sigma(s) \approx \begin{cases} (N/\pi)G_F^2 s & \text{at } s < m_W^2 \\ (N/\pi)G_F^2 m_W^2 & \text{at } s > m_W^2, \end{cases} \tag{23}$$

where $G_F = 1.17 \times 10^{-5}$ GeV^{-2} is the Fermi constant, $s(z) = 2E_\nu m_\nu(1 + z)$ is the center of mass energy squared at redshift z, E_ν is the neutrino energy at the present epoch, $m_\nu \sim 0.1 - 0.2$ eV is the assumed neutrino mass, and $N \sim 10 - 15$.

UHE neutrinos are absorbed or lose energy in collisions with relic background neutrinos whose space number density is $n_\nu = 56(1 + z)^3$ cm^{-3} and kinetic energy is $\epsilon_\nu = 3.15T(1 + z) = 5.29 \times 10^{-4}(1 + z)$ eV.

The *neutrino horizon*, i.e., the maximum redshift z_ν, from which a neutrino with the observed energy E_ν can arrive, is calculated as

$$\int_{z=0}^{z_\nu} dt\sigma_\nu(z)n_\nu(z) = 1, \tag{24}$$

where

$$dt = \frac{3}{2} t_0 (1+z)^{-5/2} dz. \quad (25)$$

At the highest neutrino energies, when $\sigma \sim \sigma_{\max} \sim (N/\pi) G_F^2 m_W^2$, $z_\nu \sim 1.5 \times 10^2$. At energies below 2×10^{11} GeV,

$$z_\nu \sim 2.5 \times 10^2 (E/10^{11}\ \text{GeV})^{-2/5}. \quad (26)$$

For energies of interest in this paper we shall use $z_\nu \sim 200$ at $E_\nu \gtrsim 10^{20}$ eV. Detectable UHE and EHE neutrinos are produced in the matter-dominated epoch.

It is interesting to note that the modulus-string model allows us to probe the earliest universe with the help of EHE neutrinos; e.g., for superconducting strings [4] the maximum redshift is $z_{\max} \sim 3$.

B. Modulus decay and neutrino spectrum

The rate of decay of a modulus into the standard model (SM) gauge bosons can be estimated as

$$\Gamma_0 \sim n_{\rm SM} \left(\frac{\alpha}{m_p}\right)^2 m^3, \quad (27)$$

where $n_{\rm SM} = 12$ is the total number of spin degrees of freedom for all SM gauge bosons, m is the modulus mass, and we assume interaction of the form [14]

$$\mathcal{L}_{\rm int} \sim \frac{\alpha}{m_p} \phi F_{\mu\nu} F^{\mu\nu}. \quad (28)$$

The mean lifetime of the modulus in its rest frame is then

$$\tau_0 \sim 8.1 \times 10^{-17} m_5^{-3} \alpha_7^{-2}\ \text{s}. \quad (29)$$

For a wide range of parameters m_5 and α, the lifetimes of moduli are short even after a large Lorentz boost. In our main scenario, the neutrino-producing moduli are born within the neutrino horizon and decay almost momentarily there.

However, in principle the redshifts $z > z_\nu$ can also contribute to the neutrino flux at $z = 0$, if the lifetime of boosted moduli is long and they can decay at $z < z_\nu$. In the analysis below we argue that such a scenario is disfavored.

The lifetimes of moduli emitted from cusps are boosted by large Lorentz factors. A modulus emitted with a Lorentz factor $\gamma_0 = k/m$ at redshift z and decaying at redshift z_d has a lifetime

$$\tau(z) \sim \tau_0 \gamma_0 \frac{1+z_d}{1+z}. \quad (30)$$

In order for neutrinos to reach the Earth, they should be produced within the neutrino horizon at redshifts $z_d \lesssim z_\nu$. Moduli emitted from cusps at $z > z_\nu$ can therefore yield observable events only if they have large enough lifetime, allowing them to survive until they reach z_ν. This gives the condition

$$\tau(z) \sim \tau_0 \gamma_0 \frac{1+z_\nu}{1+z} \gtrsim t(z_\nu) \approx t_0 (1+z_\nu)^{-3/2}, \quad (31)$$

where in the last step we used the fact that in the energy range of interest $z_\nu \lesssim z_{\rm eq}$.

For $z > z_\nu$ and using $m_5 \gtrsim 1$ and $\alpha_7 \gtrsim 1$ (which is necessary for detectable neutrino flux; see Sec. IV), we obtain

$$\gamma_0 \gtrsim \frac{t_0/\tau_0}{(1+z_d)(1+z_\nu)^{1/2}} \approx \frac{3.8 \times 10^{32}}{1+z_d}, \quad (32)$$

which is too large at any z_d.

In what follows we shall consider only cusp events occurring at $z < z_\nu < z_{\rm eq}$. There are no restrictions on the modulus lifetime in this case, except that it should be short enough for a sufficient fraction of moduli to decay before they reach the Earth. This is always satisfied in the parameter range of interest.

The decay channel relevant for the neutrino production is the decay into gluons, via the modulus-gluon interaction of the form (28). The primary gluons from the modulus decay initiate the quark-gluon cascade, which turns into hadrons, mostly in pions, and then to neutrinos.

To simplify calculations and analysis, we shall assume the neutrino production spectrum $dN/dE \propto E^{-2}$, close to the power-law approximation $E^{-1.9}$ obtained for a large mass of the decaying particle using Monte Carlo simulation and the Dokshitzer-Gribov-Lipatov-Altarelli-Parisi (DGLAP) method [24].

The neutrino spectrum from a modulus at rest is then

$$\frac{dN_\nu^*}{dE_*} \equiv \xi_\nu^*(E_*, m) \approx \frac{1}{2} f_\pi b_* \frac{m}{E_*^2}, \quad (33)$$

where m is modulus mass, E_* is neutrino energy, b_* is given in terms of the ratio of maximum $\varepsilon_*^{\max} \sim 0.1m$ and minimum $\varepsilon_*^{\min}$ neutrino energy,

$$b_* = [\ln(\varepsilon_*^{\max}/\varepsilon_*^{\min})]^{-1}, \quad (34)$$

and $f_\pi \sim 1$ and $1/2$ are the fractions of energy transferred from the modulus to pions and from pions to neutrinos, respectively.

The spectrum of low-energy neutrinos is a model-dependent feature, but generically suppression of this spectrum is provided by suppression of soft gluon emission due to the coherence effect in the parton cascade. It results in the Gaussian peak in the spectrum of pions, parents of neutrinos. We describe effects of low-energy suppression of the neutrino spectrum introducing formally the energy $\varepsilon_*^{\min}$ in Eq. (34), where the suppression starts, and refer to it as "the minimal energy," Determining the value of $\varepsilon_*^{\min}$ would require numerical calculations. Here, we shall parametrize

$$\varepsilon = \epsilon_*^{\min}/1\ \text{GeV}. \quad (35)$$

C. Lorentz boost and beaming

Emerging from a cusp segment, a modulus obtains very large Lorentz factor γ corresponding to the point of exit. The typical Lorentz factor, as it is calculated below, reaches $\gamma \sim 10^{12} - 10^{13}$. The neutrino energy E_* in the modulus rest system is boosted as

$$E = \gamma E_*(1 + \beta \cos\vartheta_*), \tag{36}$$

where $\beta = v/c$, and ϑ_* is the angle between the directions of neutrino motion and of the boost in the rest frame of the modulus.

First of all we calculate how the neutrino spectrum (33) changes under the transformation (36). For this we use the conservation of the number of particles before and after the Lorentz boost:

$$dN_*(E_*, \vartheta_*) = \frac{1}{2} b_* m \frac{dE_*}{E_*^2} \frac{d\Omega_*}{4\pi} = dN(E, E_*). \tag{37}$$

Using

$$d\Omega_* = 2\pi d\cos\vartheta_* = 2\pi \frac{dE}{\gamma\beta E_*}, \tag{38}$$

we obtain in terms of the new variables E and E_*

$$\frac{d^2N}{dE dE_*} = b_* \frac{m}{4\gamma\beta E_*^3}. \tag{39}$$

Integrating with respect to dE_* we have

$$\frac{dN}{dE} = b_* \frac{m}{8\gamma\beta} \frac{1}{E_{*\min}^2(E)}, \tag{40}$$

where the minimum neutrino energy for a fixed E is

$$E_{*\min}(E) = \begin{cases} E/[\gamma(1+\beta)] & \text{if } E \geq \gamma(1+\beta)\varepsilon_*^{\min} \\ \varepsilon_*^{\min} & \text{if } E \leq \gamma(1+\beta)\varepsilon_*^{\min}, \end{cases} \tag{41}$$

Finally, we obtain for $\beta \approx 1$ and for decay at epoch z

$$\frac{dN}{dE} \equiv \xi_\nu(E, k, z) = \frac{1}{2} \frac{b_*}{1+z} \frac{k}{E^2}, \tag{42}$$

if the neutrino energy at the present epoch is $E \geq \gamma(1 + \beta)\varepsilon_*^{\min}$. For $E \leq \gamma(1 + \beta)\varepsilon_*^{\min}$, dN/dE does not depend on the neutrino energy E:

$$\frac{dN}{dE} \equiv \xi_\nu(E, k, z) = \frac{1}{8} \frac{b_*}{1+z} \frac{k}{\gamma^2} \frac{1}{(\varepsilon_*^{\min})^2}. \tag{43}$$

In both formulas above, $k = \gamma m$ is the modulus energy.

We now briefly discuss the effect of beaming. Strong beaming of the produced particles is a remarkable feature of the cusp models, which provides interesting observational consequences. For moduli with the range of masses considered here the beaming is very strong (see Sec. II). When gravitational radiation dominates, the Lorentz factor at $z = 0$ can be estimated as $\gamma_c \approx 4.5 \times 10^{13} m_5^{1/2} \mu_{-20}^{1/2}$. When modulus radiation dominates, the Lorentz factor at z_* is $\gamma_c = \alpha^2/4\Gamma = 5 \times 10^{11} \alpha_7^2$. As a typical Lorentz factor for neutrino production one may consider that at neutrino horizon $z_\nu \sim 200$, $\gamma_c = 8.5 \times 10^{11} m_5^{1/2} \mu_{-20}^{1/2}$.

In the frame where the modulus is at rest, neutrinos are emitted isotropically. After a Lorentz boost, most of them move within a narrow cone with $\vartheta \sim 1/\gamma$ in the direction of the boost, with energies $E \sim \gamma E_*$. However, neutrinos which are emitted in the rest frame within a narrow cone with $\vartheta'_{*c} = 1/\gamma$ in the backward direction are moving after the boost within a wide angle $\vartheta \sim \pi/2$ in the direction opposite to the narrow high-energy jet and typically have very low energies $E \sim E_*/\gamma$. The total number of these neutrinos is $4\gamma^2$ times smaller than that in the high-energy jet, and they are undetectable because of their small number and low energies. The typical neutrino energies in high-energy beam is $E \sim \gamma E_*$, but low-energy neutrinos with $E \sim E_*/\gamma$ are also present there.

Formally, the minimum neutrino energy is extremely low, $E \sim \varepsilon_*^{\min}/\gamma$, but the number of such neutrinos is very small. However, when the neutrino spectrum is changing from E^{-2} at high energies to $dN/dE \propto$ const, as in Eq. (43), the detectability of neutrinos is sharply decreased, and thus $E_{\min} \approx \gamma(z)\epsilon_*^{\min}$ can be regarded as an effective low-energy end of the spectrum at epoch z. To estimate the low-energy spectrum cutoff for neutrinos generated at epoch $z_\nu \sim 200$ and observed now, we use the parametrization (35) and our estimate for the Lorentz factor at $z_\nu \sim 200$, $\gamma_c = 8.5 \times 10^{11} m_5^{1/2} \mu_{-20}^{1/2}$. Taking into account the redshift of the neutrino energy, we find $E_{\min} 4.3 \times 10^9 \epsilon m_5^{1/2} \mu_{-20}^{1/2}$ GeV. This estimate demonstrates the remarkable feature of our model: the predominant generation of the highest-energy neutrinos. A more realistic estimate of $E_{\min}$ for the diffuse neutrino flux will be made in Sec. IV C.

EHE neutrinos propagate as a jet in a cone with an opening angle $\vartheta \sim 1/\gamma$. The duration of the neutrino pulse is very short, $\tau \sim L/\gamma^3$, and all neutrinos reach the detector almost simultaneously, due to the smallness of the neutrino mass. The effective area illuminated by arriving neutrinos is much larger than the area controlled by the detector, but the simultaneous appearance of two to three showers in the field of view of a large detector is possible for some parameter values (see [4] for discussion and calculations).

Beaming is a property of all particles emitted from a cusp, in particular, gamma rays. In some models part of observed gamma-ray bursts may be produced by cosmic strings [6]. Since the total number of strings in the Milky Way is tremendously large ($N \sim 10^9$), one may expect that UHE gamma-ray bursts from the Milky Way may be observable. In fact, the rate of predicted bursts is too strongly suppressed by the beaming factor $\Omega/4\pi = 1/(4\gamma^2)$ to be detectable. The backward component is distributed within a wide solid angle and is not suppressed by this factor, but the total number of photons and their energies are too small for detection.

IV. NEUTRINO BURSTS FROM MODULI

A. Loop distribution

The predicted flux of EHE neutrinos depends on the typical length of loops produced by the string network. The typical loop sizes have been a subject of much recent debate, with different simulations [25–32] and analytic studies [33,34] yielding different answers. Here we shall adopt the picture suggested by the largest and, in our view, the most accurate string simulations performed to date [32]. According to this picture, the characteristic length of loops formed at cosmic time t is given by the scaling relation

$$L \sim \beta t, \tag{44}$$

with $\beta \sim 0.1$.

The number density of loops with lengths in the interval from L to $L + dL$ can be expressed as $n(L, t)dL$. Of greatest interest to us are the loops that formed during the radiation era ($t < t_{\rm eq}$) and still survive at $t > t_{\rm eq}$. The density of such loops is given by

$$n(L, t)dL \sim p^{-1}\zeta(\beta t_{\rm eq})^{1/2}t^{-2}L^{-5/2}dL, \tag{45}$$

where p is the string reconnection probability and $\zeta \sim 16$ is the parameter characterizing the density of infinite strings with $p = 1$, $\rho_\infty = \zeta\mu/t^2$.

The dependence of the loop density on p is somewhat uncertain and can only be determined by large-scale numerical simulations. Here we have adopted the p^{-1} dependence suggested by simple arguments in, e.g., [35,36]. The reconnection probability is $p = 1$ for ordinary cosmic strings. Its value for F- and D-strings of superstring theory has been estimated as [37]

$$10^{-3} \lesssim p \lesssim 1. \tag{46}$$

The distribution (45) applies for L in the range from the minimum length $L_{\rm min}$ to $L_{\rm max} \sim \beta t_{\rm eq}$. The lower cutoff $L_{\rm min}$ depends on whether the energy dissipation of loops is dominated by gravitational or by modulus radiation. It is given by (15) for $z < z_*$ and by (17) for $z_* < z < z_{\rm eq}$, with z_* from Eq. (20). For $z_* > z_{\rm eq}$, the dominant energy loss is gravitational radiation and Eq. (15) for $L_{\rm min}$ applies in the entire range of interest.

The string motion is overdamped at early cosmic times, as a result of friction due to particle scattering on moving strings. The overdamped epoch ends at [1]

$$t_{\rm damp} \sim (G\mu)^{-2}t_p, \tag{47}$$

where t_p is the Planck time. In the above analysis we have assumed that loops of interest to us are formed at $t > t_{\rm damp}$. The corresponding condition is

$$L_{\rm min}(t) \gtrsim \beta t_{\rm damp}. \tag{48}$$

This bound assumes that the strings have non-negligible interactions with the standard model particles, so it may not apply to F- or D-strings of superstring theory. In any case, we have verified that (48) is satisfied for parameter values that give a detectable flux of neutrinos.

B. Gravity- and moduli-dominated regimes: Restrictions imposed by z_*

The value of z_* given by Eq. (20) marks the boundary between two regimes of string evolution. In the first regime, at $z < z_*$, the string energy loss is dominated by gravitational radiation. This includes the entire relevant range of z for $z_* > z_\nu$ and the range $0 \le z \le z_*$ for $z_* < z_\nu$. We shall call it the *gravity-dominated regime*.

The second regime is dominated by the modulus radiation; we shall call it the *moduli-dominated regime*. It corresponds to the redshift interval $z_* \le z \le z_\nu$ and exists only when $z_* < z_\nu$.

It is often convenient to perform the calculations for the fixed value of z_*, considering it as a free parameter. In this case the space of three physical parameters α_7, m_5, and μ is restricted by Eq. (20) as $400\alpha_7^{-8/3}m_5^{2/3}\mu_{-20}^{2/3} = z_*$, which we will use in the form

$$\mu_{-20} = (z_*/400)^{3/2}\alpha_7^4 m_5^{-1}. \tag{49}$$

Then our calculated quantities, such as neutrino fluxes and characteristic energies, will depend on two parameters, α_7 and m_5, and the fixed value of z_*.

The value of fixed z_* characterizes "the model." One should distinguish two major classes of models: with high $z_* > z_\nu$, which corresponds to the gravity-dominated regime, and with low $z_* < z_\nu$, which includes both the gravity-dominated regime at $0 \le z \le z_*$ and the moduli-dominated regime at $z_* \le z \le z_\nu$.

C. Neutrino flux

As we argued in Sec. III B, the neutrino-producing moduli are born and decay within the neutrino horizon at $z \le z_\nu$. We shall first consider the high z_* models with $z_* > z_\nu$ (gravity-dominated regime) and then study the case $z_* < z_\nu$, which includes both the moduli-dominated regime at $z_* \le z \le z_\nu$ and the gravity-dominated regime at $0 \le z \le z_*$.

The neutrino flux can be most generally calculated as

$$J_\nu(E, z) = \frac{1}{4\pi}\int \frac{dV(z)}{1+z}d\dot{N}_b dN_X^b(k)\frac{\Omega_k}{4\pi}\frac{1}{\Omega_k r^2(z)}\xi_\nu(E, z, k), \tag{50}$$

where the proper volume for the matter-dominated epoch is

$$dV(z) = 54\pi t_0^3[(1+z)^{1/2} - 1]^2(1+z)^{-11/2}dz, \tag{51}$$

the rate of bursts is $d\dot{N}_b = n(L)dL/(L/2)$ with $n(L)dL$ being the number density of loops with length L in the interval dL [see Eq. (45)], the number of moduli dN_X^b emitted in a burst with momenta k in the interval dk is given by Eq. (6), $\Omega_k/4\pi$ is the probability that a randomly

oriented burst is directed to the observer, $\Omega_k r^2(z)$ is the area of the irradiated spot at the observer's location, and $\xi_\nu(E, z, k)$ is the spectrum of neutrinos from decay of a modulus with momentum k, given by Eqs. (42) and (43).

Integration in Eq. (50) goes over k, L, and z. For integration over k and L only lower limits are essential, and they are given by $k_{\min} = m\sqrt{mL}$ and $L_{\min}$ from Eq. (15) or Eq. (17) for the gravity-dominated and moduli-dominated regimes, respectively. In the case $z_* > z_\nu$, we have $z_{\max} = z_\nu$, while $z_{\min}$ is determined by the rate of bursts or by minimum energy of neutrino $E_{\min}(z)$ at epoch z as explained below.

Consider first the limit $z_{\min}$ imposed by the rate of bursts. The average rate of bursts $\dot{N}_b(<z)$ that occur in the redshift interval between 0 and z is a growing function of z, and we can define z_b as the redshift at which this rate is a few bursts per year. No bursts will be detected from $z \ll z_b$, so we should introduce a lower cutoff of z integration at $z_{\min} = z_b$. The rate of burst $\dot{N}_b$ is calculated in Sec. IV D and z_b is found to be small in the parameter range that we are considering here. Hence, the condition $z > z_b$ does not yield a significant constraint for the z integration in Eq. (50).

Another constraint to consider is that the energy E of neutrinos should be above the minimal energy, $E > E_{\min}(z) = \gamma_c(z)\varepsilon_*^{\min}/(1+z)$, where $\gamma_c(z) = \frac{1}{4} \times [mL_{\min}(z)]^{1/2}$ is the characteristic Lorentz factor for loops of minimal length $L_{\min}(z)$ at epoch z. For the gravity-dominated regime we are considering here

$$\gamma_c(z) = 4.5 \times 10^{13} m_5^{1/2} \mu_{-20}^{1/2} (1+z)^{-3/4}. \quad (52)$$

To proceed, it will be convenient to use z_* in place of the string tension μ as a free parameter. With the aid of Eq. (49) we have

$$E_{\min}(z) = E_0 \alpha_7^2 (z_*/z_\nu)^{3/4} (1+z)^{-7/4}, \quad (53)$$

where

$$E_0 = 2.7 \times 10^{13} \varepsilon \text{ GeV}, \quad (54)$$

and ε is the parametrization factor introduced in Eq. (35). The lower bound of z integration $z_{\min}$ can now be found as the value of z for which $E_{\min}(z) = E$,

$$1 + z_{\min}(E) = (E_0/E)^{4/7} \alpha_7^{8/7} (z_*/z_\nu)^{3/7}. \quad (55)$$

Integrating Eq. (50) over z from $z_{\min}(E)$ to z_ν, since we assumed above $z_* > z_\nu$, we obtain

$$E^2 J_\nu(E) = 2.5 \times 10^{-9} p^{-1} \alpha_7^2 m_5^{-1/2} \left(\frac{z_\nu}{200}\right)^{1/2} \times \left[1 - \left(\frac{1+z_{min}(E)}{1+z_\nu}\right)^{1/2}\right] \text{GeV/cm}^2\,\text{s}\,\text{sr}. \quad (56)$$

The calculated flux for a "normalizing" set of parameters $p = 1$ (ordinary strings) and $\alpha_7 = m_5 = z_*/z_\nu = 1$ is shown in Fig. 1 by curve "theor. 3." This flux is low and detectable only by SKA. The largest flux in Fig. 1 is presented by curve "theor. 1" for the parameters $p = 1$, $\alpha_7 = 2$, $m_5 = 0.1$, $z_*/z_\nu = 1$. It is close to the upper limit shown by curve "E^{-2} cascade," and is detectable by JEM-EUSO, LOFAR, and SKA. Here and everywhere below we assume $\varepsilon = 1$.

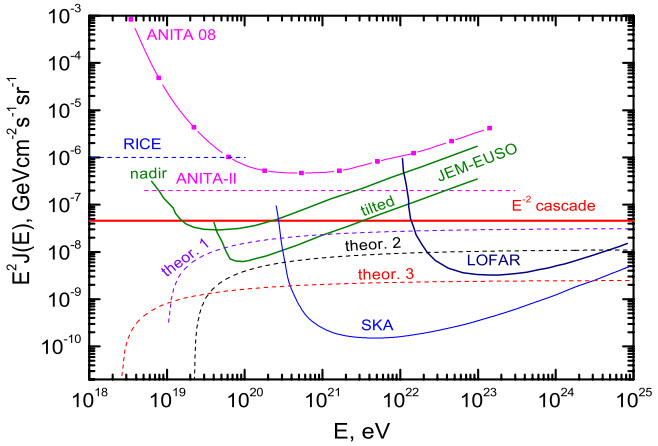

FIG. 1 (color online). Calculated neutrino fluxes compared with existing upper limits, the Antarctic Impulse Transient Antenna–II (ANITA-II), Radio Ice Cerenkov Experiment (RICE), ANITA 08, and with sensitivities of projects, Japanese Experiment Module–Extreme Universe Space Observatory (JEM-EUSO), Low Frequency Array (LOFAR), and Square Kilometer Array (SKA). Line "E^{-2} cascade" presents the upper limit for *cosmogenic* neutrinos [40]. Curve "theor. 3" gives the predicted neutrino flux for the gravity-dominated regime with a normalizing set of parameters $p = 1$ (ordinary strings), and $\alpha_7 = m_5 = z_*/z_\nu = 1$. This flux is detectable only by SKA. Curve "theor. 2" corresponds to the superstring-motivated example in the gravity-dominated regime (see Sec. IV F) with $p = 1$, $z_*/z_\nu = 1$, $\alpha_7 = 3$, and $m_5 = 4$. This flux is detectable by SKA and LOFAR. Increasing further the product $\alpha_7^2 m_5^{-1/2}$ the flux can be made detectable by JEM-EUSO, though increasing of α_7 should be limited, because of increasing of $E_{\min}$ due to this factor. The curve "theor. 1" with parameters $p = z_*/z_\nu = 1$, $\alpha_7 = 2$, and $m_5 = 0.1$ gives the flux detectable by all three future instruments SKA, LOFAR, and JEM-EUSO. In the case of the moduli-dominated regime with parameters considered in Sec. IV G as $\alpha_7 = 2$, $m_5 = 0.1$, and $z_* = 100$, neutrino flux is observable by all three detectors, SKA, LOFAR, and JEM-EUSO.

The maximum energy of neutrinos is determined by $E_{\max} \sim 2\gamma\epsilon_*^{\max}$ at generation and can be extremely large, but the flux of these neutrinos is suppressed as E^{-2}.

We shall now consider the low z_* models with $z_* \le z_\nu$, and calculate first the neutrino flux generated in the redshift interval $z_* \le z \le z_\nu$, where energy losses are moduli-dominated. Then we calculate flux in the interval $0 \le z \le z_*$, where the gravitational radiation dominates.

For the interval $z_* \le z \le z_\nu$ and fixed z_*, the neutrino flux is calculated using Eq. (50) and the parameter restriction in the form $\mu_{-20}^{2/3} = (z_*/400)\alpha_7^{8/3} m_5^{-2/3}$. As a result we have

$$E^2 J_\nu(E) = \frac{1}{2} K p^{-1} \alpha_7^2 m_5^{-1/2} (1+z_*) \int_{z_{\min}(E)}^{z_\nu} dz (1+z)^{-3/2}, \tag{57}$$

with $K = 1.8 \times 10^{-10}$ GeV/cm^2 s sr.

The lower limit of integration in Eq. (57) is obtained as above from $E_{\min}(z) = \gamma_c(z)\varepsilon_{\min}/(1+z)$. Using the condition $E \geq E_{\min}(z)$ and $z_{\min} \geq z_*$ one obtains

$$z_{\min}(E) = \begin{cases} z_* & \text{at } E \geq \tilde{E}_{\min} \\ (E/E_0)^{-2/3} \alpha_7^{4/3} z_*^{1/3} & \text{at } E_{\min} \leq E \leq \tilde{E}_{\min} \\ z_\nu & \text{at } E \leq E_{\min}, \end{cases} \tag{58}$$

with $E_{\min} = 1.3 \times 10^{18} \varepsilon \alpha_7^2 (z_*/50)^{1/2}$ eV, $\tilde{E}_{\min} = 1 \times 10^{19} \varepsilon \alpha_7^2 (50/z_*)^2$ eV, and $E_0 = 5 \times 10^{20} \varepsilon$ eV. Finally we have

$$E^2 J_\nu(E) = K p^{-1} \alpha_7^2 m_5^{-1/2} \frac{1+z_*}{(1+z_\nu)^{1/2}} \left[\left(\frac{1+z_\nu}{1+z_{\min}} \right)^{1/2} - 1 \right]. \tag{59}$$

Using in Eq. (59) $z_{\min}(E) = z_*$ at $E \geq \tilde{E}_{\min}$ [see Eq. (58)] one finds the high-energy (HE) asymptotic of the flux in the moduli-dominated regime

$$E^2 J_\nu(E) = 1.8 \times 10^{-10} p^{-1} \alpha_7^2 m_5^{-1/2} (1+z_*)^{1/2} \times \left[1 - \left(\frac{1+z_*}{1+z_\nu} \right)^{1/2} \right] \text{GeV cm}^{-2} \text{s}^{-1} \text{sr}^{-1}, \tag{60}$$

valid at $E \gtrsim \tilde{E}_{\min}$.

We have to add also the neutrino flux generated in the interval $0 \leq z \leq z_*$ where the gravitational energy losses dominate. In this case $L_{\min}$ is given by Eq. (15). For the HE asymptotic one finds

$$E^2 J_\nu(E) = 1.8 \times 10^{-10} p^{-1} \alpha_7^2 m_5^{-1/2} (1+z_*)^{1/2} \times \text{GeV cm}^{-2} \text{s}^{-1} \text{sr}^{-1}. \tag{61}$$

For an easily understandable reason, the HE asymptotic here is $(z_*/z_\nu)^{1/2}$ lower than in the case $z_* > z_\nu$ given by Eq. (56). Less trivial is the coincidence of the HE asymptotic in the gravitational regime $(0, z_*)$ given by Eq. (61) and in the moduli-dominated regime (z_*, z_ν) given by Eq. (60). It is explained by the fact that dominant contributions in both cases are given by epochs with redshift z_*. The general conclusion about neutrino production is therefore increasing the flux with growth of z_* until it reaches z_ν. Thus, the high z_* models predict the largest neutrino fluxes.

Apart from this, more efficient neutrino detection in high z_* models, follows from a lower cutoff energy $E_{\min}$. Indeed, the minimal energy of neutrinos for both regimes $(0, z_*)$ and (z_*, z_ν) is determined by the same expression

$$E_{\min}(z_*) = \frac{\gamma_c(z_*)}{1+z_*} \varepsilon_*^{\min} = \frac{1}{4} \frac{\alpha^2}{\Gamma} \frac{\varepsilon_*^{\min}}{1+z_*}, \tag{62}$$

while for the gravity-dominated regime with $z_* > z_\nu$ it is determined by z_ν as

$$E_{\min}(z_\nu) = \frac{\gamma_c(z_\nu)}{1+z_\nu} \varepsilon_*^{\min}. \tag{63}$$

Increasing z_* in Eq. (62) we decrease $E_{\min}$, which is favorable for detection by JEM-EUSO.

One may also see that the moduli-dominated regime gives a subdominant effect as compared with the gravity-dominated one at $z_* > z_\nu$.

D. The rate of bursts

The rate of bursts is not a physically measured quantity, but it can serve as an indicator of detectability of the burst radiation.

The rate of cusp bursts with their cones of radiation directed to the observer is given by

$$\dot{N}_b = \int \frac{dV(z)}{1+z} \frac{n(L,z)}{L/2} dL \frac{\Omega}{4\pi}, \tag{64}$$

where $dV(z)$ and $n(L)dL$ are the same as in Eq. (50). The quantity $\Omega/4\pi$ gives the probability for the observer to be located within the cone of the cusp radiation. Such a location does not guarantee detection of this radiation, because the area of irradiated spot Ωr^2 is much bigger than the size of the solar system, but a too low rate of bursts means that the signal is undetectable. To calculate $\Omega \approx \pi \vartheta^2$ we use $\vartheta \sim (k_c L)^{-1/3}$ [see the discussion above Eq. (A23) in the Appendix for details].

We calculate the rate of bursts for $z < z_*$, when gravitational radiation dominates. The rate integrated from $z = 0$ up to redshift z is given by

$$\dot{N}_b(\leq z) = \frac{54\pi}{7} 2^{4/3} p^{-1} \zeta \beta^{1/2} \frac{(t_{\text{eq}}/t_0)}{(\Gamma G \mu)^{7/2}} \frac{1}{m t_0^2}$$
$$I(z) = 1.1 \times 10^7 \mu_{-20}^{-7/2} m_5^{-1} I(z) \text{ yr}^{-1}, \tag{65}$$

where

$$I(z) = \int_0^z dz' [(1+z')^{1/2} - 1]^2 (1+z')^{7/4}. \tag{66}$$

Numerical values of $I(z)$ are shown in Table I.

In Sec. IV C $z_{\min} \equiv z_b$ is defined from condition $\dot{N}_b(\leq z_b)$ as a few per year. From Table I and Eq. (65) one can see that the rate of bursts is large enough even at redshift as

TABLE I. Numerical values of integral $I(z)$.

z	0.1	0.5	1.0	2.0
$I(z)$	9.12×10^{-5}	0.015	0.165	1.99

small as 0.1, and thus the condition $z > z_b$ does not impose a significant constraint for the integration of Eq. (50) over z.

E. Cascade upper bound

An upper bound on the neutrino flux follows from the observed diffuse HE gamma-ray background, since neutrino production via pion/kaon decays is accompanied by high-energy electron and photon production. These electrons and photons, interacting with CMB and extragalactic background light photons, produce an electromagnetic cascade, whose energy density $\omega_{\rm cas}$ must not exceed that of the observed diffuse gamma radiation. This results in the upper limit on the diffuse neutrino flux [38]. With the assumption of the E^{-2} generation spectrum of neutrinos the cascade upper limit can be written as

$$E^2 J_\nu(E) \le \frac{c}{4\pi} \frac{\omega_{\rm cas}^{\rm max}}{\ln(E_{\rm max}/E_{\rm min})}, \tag{67}$$

where $E_{\rm max}$ and $E_{\rm min}$ are the maximum and minimum neutrino energies, respectively, and $\omega_{\rm cas}^{\rm max}$ is the maximum cascade energy density allowed by observation of the isotropic diffuse gamma radiation.

According to recent Fermi–Large Area Telescope observations [39] this energy density is $\omega_{\rm cas}^{\rm max} = 5.8 \times 10^{-7}$ eV/cm^3, as it follows from the analysis [40,41]. This limit results from a comparison of the cascade spectrum at 100 GeV with the Fermi data, while the lower energies give a weaker limit. For our case we assume that cosmological epochs with redshifts $z \ge z_{\rm cas}$, when gamma rays with $E_\gamma > 30$ GeV are absorbed, make a negligible contribution to the obtained upper limit. One can estimate $z_{\rm cas}$ in the following way. At $z = 0$ a very sharp absorption of gamma rays on CMB occurs at $E_\gamma^{\rm abs}(0) \approx 100$ TeV. At epoch z this energy is $(1 + z)$ lower. Taking into account the redshift of these photons, we estimate $z_{\rm cas}$ as $z_{\rm cas} \sim (E_\gamma^{\rm abs}/E_\gamma)^{1/2} \sim 60$.

The energy density for the electromagnetic cascade radiation resulting from modulus decays can be expressed as

$$\omega_{\rm cas} = \frac{1}{2} f_\pi \int \frac{dt}{(1+z)^4} \frac{n(L,z)dL}{L/2} N(k) k dk, \tag{68}$$

where $f_\pi \sim 1$ and $1/2$ are the fractions of energy transferred from the modulus to pions and from pions to electrons and photons, respectively, dt is given by Eq. (25), the density of the loops $n(L)$ is given by Eq. (45), and the number of moduli emitted per burst $N(k)$ is given by Eq. (6). The limits of integration in Eq. (68) are as follows: $z_{\rm min} = 0$, $z_{\rm max} = z_{\rm cas} \sim 60$, $k_{\rm min} = (1/4)m\sqrt{mL}$, and $L_{\rm min}$ is given by Eqs. (15) and (17) for the cases $z_* > z_{\rm cas}$ and $z_* < z_{\rm cas}$, respectively.

Consider first the case $z_* > z_{\rm cas}$, when gravitational radiation dominates. Performing the integration we obtain

$$\omega_{\rm cas} = 9 \times 2^{-1/3} p^{-1} \zeta \beta^{1/2} \Gamma^{-2} \frac{(t_{\rm eq}/t_0)^{1/2}}{(t_0 m)^{1/2}} \alpha^2 \frac{m_{Pl}^2}{t_0^2} (1+z_{\rm cas})^{1/2}$$
$$= 5.8 \times 10^{-9} p^{-1} \alpha_7^2 m_5^{-1/2} (z_{\rm cas}/60)^{1/2} \ {\rm eV/cm^3}. \tag{69}$$

For $z_* < z_{\rm cas}$ we have to integrate over the interval $0 \le z \le z_*$, where gravitational radiation dominates, and over interval $z_* \le z \le z_{\rm cas}$, where moduli radiation prevails. For the first case (gravity-dominated regime at $0 \le z \le z_*$) one obtains

$$\omega_{\rm cas} = 4.7 \times 10^{-9} p^{-1} \alpha_7^2 m_5^{-1/2} (z_*/40)^{1/2} \ {\rm eV/cm^3}. \tag{70}$$

For the second case (moduli-dominated regime at $z_* \le z \le z_{\rm cas}$) we have using Eq. (49)

$$\omega_{\rm cas} = 4.7 \times 10^{-9} p^{-1} \alpha_7^2 m_5^{-1/2} (z_*/40)^{1/2} \times [1 - (z_*/z_{\rm cas})^{1/2}] \ {\rm eV/cm^3}. \tag{71}$$

Note that this is the same as (70), apart from the last factor. The reason is that in both cases the main contribution to z integration comes from $z \sim z_*$, like in case already discussed for neutrino fluxes.

For reasonable values of z_*, all three $\omega_{\rm cas}$ given by (69)–(71) are less than maximally allowed $\omega_{\rm cas}^{\rm max} = 5.8 \times 10^{-7}$ eV/cm^3.

Two remarks about the cascade limit for our model are now in order.

This limit is not strictly enforced because cascade production occurs at very large redshifts, while $\omega_{\rm cas}$ is constrained mainly due to the highest-energy cascade photons with $E \approx 100$ GeV (see Fig. 1 in [40]). These photons are absorbed by the extragalactic background light at earlier cosmological epochs, and therefore in cosmic string models, where the main part of the cascade energy density is produced at large redshifts, the constraint on $\omega_{\rm cas}$ is weaker and values higher than 5.8×10^{-7} eV/cm^3 are allowed. Therefore, neutrino fluxes above the E^{-2} cascade upper limit taken from [40] and shown in Fig. 1 are not necessarily excluded.

One may also expect that beaming of cascades may reduce the efficiency of the cascade limit. The calculation of beam widening in the ambient magnetic field shows that narrow beaming survives only for very weak magnetic fields of order 10^{-15} G.

F. Superstring-motivated example for high z_* model with $z_* > z_\nu$

Because of the simplifying assumptions adopted in this paper, we cannot reliably determine the domain in the parameter space of α, m, and $G\mu$, which yields detectable fluxes of EHE neutrinos.

Instead, we shall discuss some illustrative examples of parameter choices, for which neutrino detection in future experiments is possible. Among such projects we shall consider detectors aimed at the highest-energy neutrinos

above 10^{20} eV: JEM-EUSO [42], Anita-II [43], LOFAR [44,45], SKA [44,46], and the Lunar Orbit Radio Detector (LORD) [47]. JEM-EUSO is based on space detection of fluorescent light from the showers in the atmosphere. All others are based on radio detection of the showers due to the Askarian effect [48]. The sensitivities of three of these experiments, JEM-EUSO (expected to be launched in 2015), LOFAR, and SKA, are shown in Fig. 1.

First we shall consider a superstring-motivated example for cosmic strings evolving in the gravity-dominated regime, assuming that $z_* > z_\nu$. We fix plausible parameters, both for strings and for particle physics. Specifically, we consider the large volume string compactification model [13], which is characterized by an intermediate string scale $m_s \sim 10^{11}$ GeV and a TeV-scale supersymmetry breaking. The hierarchy between the Planck and supersymmetry breaking scales in this model is due to an exponentially large volume of the compact extra dimensions, $V_{\rm comp} \equiv \mathcal{V} l_s^6$, where $\mathcal{V} \sim 10^{15}$ and $l_s \sim m_s^{-1}$ is the string length scale.

Apart from the volume modulus, which has gravitational-strength couplings to ordinary matter, the other Kahler moduli have large couplings of the order [14]

$$\alpha \sim \sqrt{\mathcal{V}}. \tag{72}$$

With $\mathcal{V} \sim 10^{15}$, we have $\alpha \sim 10^{7.5}$.

The modulus masses are given by [14]

$$m \sim \frac{ln\,\mathcal{V}}{\mathcal{V}} m_p. \tag{73}$$

It is useful to parametrize m in terms of α. Since we are interested in $\alpha \sim 3 \times 10^7$, the factor $ln\,\mathcal{V}$ can be replaced by 35. Hence, we obtain for the mass

$$m \sim 35 m_p \alpha^{-2}. \tag{74}$$

For $\alpha \sim 3 \times 10^7$ we have $m \sim 4 \times 10^5$ GeV, and we fix $\mu_{-20} \sim 10$, to ensure $z_* > z_\nu$. The last condition means choosing the basic cosmic string parameter, the symmetry breaking string scale $\eta = \sqrt{\mu} \sim 3.9 \times 10^9$ GeV, i.e., $G\mu \sim 1 \times 10^{-19}$. With this choice of parameters, z_* from Eq. (20) is given by $z_* \approx 250$; i.e it is larger than $z_{\rm cas}^{\rm max} \sim 60$ and than the neutrino horizon $z_\nu \sim 200$. For this case, the neutrino flux is given by Eq. (56) and the cascade energy density by Eq. (69). With the parameters α_7 and m_5 as indicated above, the neutrino flux is $E^2 J(E) = 1.3 \times 10^{-8} p^{-1}$ GeV/cm^2 s sr and the cascade energy density is $\omega_{\rm cas} \approx 2.6 \times 10^{-8} p^{-1}$ eV/cm^3.

This neutrino flux is shown in Fig. 1 by the curve "theor. 2". It is detectable by LOFAR and SKA, but not by JEM-EUSO.

We can modify this model choosing parameters providing a larger neutrino flux. For this we fix $\alpha_7 = 2$, $m_5 = 0.1$ and keep $z_* = 250$, i.e., $\mu_{-20} \approx 80$ and $\eta \approx 1 \times 10^{10}$ GeV. The cascade energy density, $\omega_{\rm cas} = 7.3 \times 10^{-8} p^{-1}$ eV/cm^3, is safely below $\omega_{\rm cas}^{\rm max}$. This model satisfies the restrictions obtained in [12], and in fact we can further increase the flux by decreasing m_5. At the high-energy limit the calculated neutrino flux is given by $E^2 J_\nu(E) \approx 3.2 \times 10^{-8} p^{-1}$ GeV/cm^2 s sr. This flux is shown in Fig. 1 by curve theor. 1; it is detectable by JEM-EUSO, LOFAR, and SKA.

G. An illustrative example for low z_* model with $z_* < z_\nu$

Let us now assume that $z_* < z_\nu$. Then, in the redshift interval $z_* \le z \le z_\nu$ the modulus radiation dominates. In the remaining interval $0 \le z \le z_*$ the gravitational energy losses are dominant. The total neutrino flux is given by the sum of fluxes generated from both intervals. A value of z_* fixes a model. Here we try to find a model with a detectable neutrino flux.

The neutrino flux from the moduli-dominated interval (z_*, z_ν), in the HE asymptotic regime, is given by Eq. (60). This equation becomes valid just above the low-energy steepening, i.e., at

$$E \ge \tilde{E}_{\rm min} = 1 \times 10^{19} \alpha_7^2 (50/z_*)^2 \text{ eV}. \tag{75}$$

For the flux from the gravity-dominated interval $(0, z_*)$, the HE asymptotic is given by Eq. (61), with a low-energy cutoff approximately at the same energy as above. Summing up both components, we obtain

$$E^2 J_\nu(E) = 1.8 \times 10^{-10} p^{-1} \alpha_7^2 m_5^{-1/2} (1+z_*)^{1/2} \times \left[2 - \left(\frac{1+z_*}{1+z_\nu}\right)^{1/2}\right] \text{GeV cm}^{-2}\,\text{s}^{-1}\,\text{sr}^{-1}. \tag{76}$$

To maximize the flux without strongly increasing the low-energy steepening threshold $\tilde{E}_{\rm min}$ given by Eq. (75), one can use the parameters $\alpha_7 = 2$, $m_5 = 0.1$, and $z_* = 100$. As a result we obtain $\tilde{E}_{\rm min} = 1 \times 10^{19}$ eV and $E^2 J_\nu = 2.9 \times 10^{-8}$ GeV cm^{-2} s^{-1} sr^{-1}, close to the upper limit "E^{-2} cascade" in Fig. 1. This flux is detectable by JEM-EUSO, LOFAR, and SKA. The cascade energy density does not exceed $\omega_{\rm cas}^{\rm max}$.

For cosmic F- and D-strings, the p^{-1} factor alone can increase the flux and $\omega_{\rm cas}$ to and above the "E^{-2} cascade limit", keeping $E_{\rm min}$ unchanged.

H. EHE neutrino detection

The calculated EHE neutrino fluxes are shown in Fig. 1, together with the existing upper limits from ANITA 08 [43], ANITA-II [43], and RICE [49], and with the sensitivity of the proposed experiments—JEM-EUSO [42] (to be launched in 2015), LOFAR [45], and SKA [46]. The predicted fluxes are presented for the gravity-dominated regime with $z_* > z_\nu$. As is discussed in Sec. IV G in the moduli-dominated regime the neutrino fluxes can be also detectable. The characteristic feature of all models is very high minimal energy of neutrinos in spectrum $E_{\rm min}$. Because of this, neutrino fluxes in some models are undetectable by JEM-EUSO.

In all cases neutrino fluxes and cascade energy density are scaled by factor $p^{-1}\alpha_7^2 m_5^{-1/2}$. The quantity $\alpha_7^2 m_5^{-1/2}$ alone can be increased by factor 10–30. In our models neutrinos are produced at large redshifts, while $\omega_{\rm cas}^{\rm max} = 5.8\times10^{-7}$ eV/cm^3 is obtained mainly due to observation of 100 GeV photons [40], which have a local origin. Increasing the value of α_7 is limited since $E_{\rm min}$ is usually proportional to α_7^2 and these high-energy neutrinos become undetectable by JEM-EUSO. The quantity p^{-1} can be easily increased by factor 10^3 for cosmic F- and D-strings. This factor is limited by $\omega_{\rm cas}$ only; $E_{\rm min}$ does not depend on p^{-1}.

The characteristic feature of our model is the production of EHE neutrinos due to tremendously large Lorentz factors. The neutrino-induced gigantic showers in the air or lunar regolith produce a strong signal reliably detectable in optical and radio emissions. The signature of EHE neutrinos with energies above 10^{21}–10^{22} eV is given by this energy scale, which is inaccessible for astrophysical sources.

This model has another signature, already discussed in [4]: the simultaneous appearance of a few showers in the field of view of a detector. It is due to neutrino propagation in the form of a very narrow jet and to the absence of time delay in neutrino arrival, because of the tremendously large neutrino Lorentz factors $\Gamma_\nu = E_\nu/m_\nu$. Compared to the case of superconducting strings in [4], the rate of multiple showers is strongly suppressed by higher energies of neutrinos, being partly compensated by the greater target mass of gigantic radio detectors. We present some brief estimates below.

The number of detected neutrinos from a jet in the detector target is given by

$$N_\nu^{\rm det}(>E) = \frac{\sigma_{\nu N}(>E)}{m_N} M_{\rm det} F_\nu(>E), \tag{77}$$

where $\sigma_{\nu N}(>E)$ is the neutrino-nucleon cross section for neutrinos with energies greater than E, $M_{\rm det}$ is the target mass for the largest radio detectors, and $F_\nu(>E)$ is the fluence of neutrinos with energy greater than E in a jet from a source at redshift z. The fluence is calculated as

$$F_\nu(>E) = \int dk N_X^b(k) \frac{\xi_\nu(k,z,>E_{\rm min})}{\Omega_k r^2}, \tag{78}$$

where $E_{\rm min}$ is the minimum neutrino energy for a source at redshift z. In numerical estimates we shall use $\sigma_{\nu N} \sim 1\times10^{-31}$ cm^2 and $M_{\rm det}\sim 10^{21}$ g.

For the gravity-dominated regime, standard calculations give the following expression for the neutrino fluence from a loop of length $L_{\rm min}$ at redshift z:

$$F_\nu(>E) = \frac{\alpha^2}{3\pi 2^{5/3}} \frac{f_\pi}{b_*} \frac{\Gamma^{3/2}(G\mu)^{7/2}}{(t_0 m)^{1/2}} \times \frac{1}{[(1+z)^{1/2}-1]^2(1+z)^{9/4}} \frac{m}{E_{\rm min}} m_{Pl}^2, \tag{79}$$

where for $z<1$ $E_{\rm min} = 4.5\times10^{22} m_5^{1/2}\mu_{-20}\varepsilon$ eV. Estimating fluence for the illustrative case parameters $\alpha = 3\times10^7$, $m = 4\times10^5$ GeV, $\mu_{-20}=10$, and using $z\sim1$ and $E_{\rm min}\sim10^{13}$ GeV, we obtain $F_\nu \sim 3\times10^{-18}$ cm^{-2}. The number of neutrinos detected per burst is calculated as $N_\nu^{\rm det}\sim 2\times10^{-4}\mu_{-19}^3$. The fact that $N_\nu^{\rm det}\ll 1$ shows that practically all detected neutrinos are single. This is mostly due to the large value of $E_{\rm min}$ in the gravity-dominated regime.

The situation is different for the moduli-dominated regime at $z_*\le z\le z_\nu$. The fluence from a loop with $L\sim L_{\rm min}$ at redshift z_* is given by

$$F_\nu(>E) = \frac{2^{-2/3}}{6\pi}\frac{f_\pi}{b_*}(G\mu)^3 \times \frac{1}{(1+z_*)^{3/2}[(1+z_*)^{1/2}-1]^2}\alpha^4\frac{m_{Pl}^2}{Et_0}. \tag{80}$$

For the model with $\alpha_7=10$, $m_5=1$, and $z_*=40$, which yields the electromagnetic cascade flux at the energy density bound $\omega_{\rm cas}^{\rm max}$, and assuming the neutrino energy $E = 1\times10^{20}$ eV, we obtain numerically $F_\nu(>E) = 6.2\times10^{-15}$ cm^{-2}, and the mean number of neutrinos detected in a burst is $\bar N_\nu^{\rm det}\sim 0.4$. The Poisson probability to detect simultaneously $n=2$ neutrinos at average $\bar N = 0.4$ is 0.054.

V. CONCLUSIONS

Production of high-energy particles is a natural feature and one of the signatures of topological defects, including cosmic strings. It provides a method of searching for, e.g., cosmic strings, which complements other methods, based on the gravitational effects of strings, such as structure formation, CMB data, gravitational radiation, gravitational lensing, and others. The strongest current bounds on strings with a symmetry breaking energy scale $\eta=\sqrt{\mu}$ are given by $G\mu\lesssim10^{-7}$ due to lensing effect [50] and $G\mu\lesssim4\times10^{-9}$, due to the millisecond pulsar observations [51]. With more advanced gravitational wave detectors, the bound is expected to improve to $G\mu\sim10^{-12}$ [35,52]. On the other hand, UHE particles can be detected from strings with $G\mu$ values as small as $\sim10^{-20}$.

Cosmic strings can arise from a symmetry breaking phase transition in the early universe. Fundamental strings of superstring theory can also play the role of cosmic strings in some models.

A characteristic feature of the string dynamics is the periodic appearance of cusps, where very large Lorentz factors are reached for brief periods of time. Particle emission from a cusp segment results in extremely high particle energies. Astrophysical sources, at the present level of knowledge, cannot accelerate particles to energies above 10^{21}–10^{22} eV, with the maximum neutrino energy an order of magnitude lower. Thus, detection of neutrinos with $E\gtrsim10^{21}$ eV would be a signature of top-down models, with the string-cusp model as a plausible candidate. An additional

signature of this model is neutrino emission in the form of a narrow jet with simultaneous detection of two or more neutrinos possible in the field of view of the detector. However, this possibility exists only for some values of model parameters and only for large detectors.

EHE neutrino astronomy with $E \gtrsim 10^{21}$ eV can probe high-energy processes in the universe up to redshifts $z_\nu \sim 200$. At the same time these neutrinos have a large interaction cross section with nucleons, $\sigma_{\nu N} \sim 1 \times 10^{-31}$ cm^2, favorable for detection.

Moduli are produced near cusps of oscillating string loops, where the characteristic frequency of string motion exceeds the modulus mass m. These particles are emitted from a string segment with a Lorentz factor $\gamma_c \sim \sqrt{mL}/4$, where L is the length of the loop. Moduli and the products of their decays move as a jet with an opening angle $\vartheta_c \sim \gamma_c^{-1}$. A modulus decays into two gluons, which initiate a quark-gluon cascade, which turns into hadrons, mostly pions, and then to neutrinos. We assume that the neutrino spectrum in the rest frame of the modulus is $\propto E_*^{-2}$, where E_* is the neutrino energy in this frame. We adopted this spectrum in order to simplify the analysis and to obtain transparent analytic results. In fact the neutrino spectrum is not power law, and has a flattening at a low energy $\epsilon_*^{\min}$, which we call the minimum energy. This spectrum is Lorentz boosted, as described in Sec. III C, and the boosted spectrum also has a flattening at energy $E_{\min} \sim \gamma_c \epsilon_*^{\min}$. This energy can be considered as an effective low-energy cutoff of the spectrum, because at $E < E_{\min}$ the detectability of neutrinos is noticeably reduced.

Given the length distribution of loops at epoch z and the spectrum of moduli emitted from a loop of a given length, it is possible to calculate the neutrino flux $E^2 J_\nu(E)$, the cascade energy density $\omega_{\rm cas}$, which provides an upper limit on the neutrino flux (see Sec. IV E), and the cutoff energy $E_{\min}$ in the neutrino spectrum. The results are given in terms of three free parameters $\alpha_7 = \alpha/10^7$, $m_5 = m/10^5$ GeV, and $\mu_{-20} = G\mu/10^{-20}$. Another important parameter is the redshift of the neutrino horizon, $z_\nu \sim 200$.

The results of these calculations critically depend on the redshift $z_* \approx 400 \alpha_7^{-8/3} m_5^{2/3} \mu_{-20}^{2/3}$. This redshift separates two regimes in the string evolution: the gravity-dominated regime at $z \le z_*$, when gravitational energy losses are dominant, and the moduli-dominated regime at $z \ge z_*$, when modulus radiation energy losses dominate.

Apart from this selective role, fixing the value of z_* gives a constraint in the parameter space $(\alpha_7, m_5, \mu_{-20})$, in the form $z_*(\alpha_7, m_5, \mu_{-20}) = z_*'$, where z_*' is the fixed z_* value. This reduces the number of free parameters to two (at the fixed z_*), which we choose as α_7 and m_5. As a result all calculated fluxes $E^2 J_\nu(E)$ and energy density $\omega_{\rm cas}$ scale (at fixed z_*) as $p^{-1} \alpha_7^2 m_5^{-1/2}$.

In our calculations the fixed value of z_* plays the role of the most important parameter, which determines what we call "the model." The high z_* models, defined as $z_* > z_\nu$, correspond to the gravity-dominated regime in the whole allowed interval of redshifts $(0, z_\nu)$. The low z_* models, defined as $z_* < z_\nu$, are characterized by two regimes: the gravity-dominated one at $0 \le z \le z_*$ and the moduli-dominated one at $z_* \le z \le z_\nu$, with approximately equal neutrino fluxes. The total neutrino flux is increasing with growth of z_* until it reaches z_ν, and models with $z_* \ge z_\nu$ give the largest flux. This growth of flux with z_* is accompanied by a decrease of $E_{\min}$ [see Eq. (62)], which is favorable for neutrino detection by JEM-EUSO.

Three theoretical curves in Fig. 1 illustrate different cases of neutrino detectability for the gravity-dominated regime at $z_* \ge z_\nu$. The predicted flux is detectable by SKA only in case of a normalizing parameter set $p = \alpha_7 = m_5 = z_*/z_\nu = 1$ (curve "theor. 3"). The flux is detectable by LOFAR and SKA in case of $p = z_*/z_\nu = 1$, $\alpha_7 = 3$, and $m_5 = 4$ (curve "theor. 2"). The flux is detectable by all three detectors JEM-EUSO, LOFAR, and SKA if $p = z_*/z_\nu = 1$, $\alpha_7 = 2$, and $m_5 = 0.1$ (curve "theor. 1").

We considered the above "ordinary" strings with $p = 1$. For cosmic superstrings with reconnection probability $p < 1$, the neutrino flux increases by a factor p^{-1} without increasing $E_{\min}$, and is detectable for a wider range of model parameters.

The cascade upper limit on neutrino flux in Fig. 1 (E^{-2} curve) is given for cosmogenic neutrinos from [40]. It is based on maximum energy density $\omega_{\rm cas}^{\max}$ allowed by Fermi data [39]. For the considered model with the dominant contribution from large redshifts this upper limit is higher because of 100-GeV-neutrino absorption. Therefore, allowed neutrino fluxes can be further increased.

The remarkable feature of moduli-produced strings is strong beaming. The Lorentz factor at $z = z_\nu$ in the gravity-dominated regime and at z_* in the moduli-dominated regime is $\Gamma \sim 10^{12}$. The corresponding angle of a beam is $\vartheta \sim \Gamma^{-1} \sim 10^{-12}$. Neutrinos with these tremendous energies arrive simultaneously at a detector and can produce simultaneously two or more showers in the field of view of the detector. The estimates made in Sec. IV H show that such events are rare due to very high energies of neutrinos.

ACKNOWLEDGMENTS

The authors are grateful to Peter Gorham for valuable correspondence and to Askhat Gazizov for preparing the figure and for useful discussions. The work by E. S. and A. V. was supported in part by the National Science Foundation under Grant No. PHY-0855447.

APPENDIX

In this section we shall derive the modulus radiation spectrum in more detail. In a flat background, i.e., $g_{\mu\nu} = \eta_{\mu\nu} = \mathrm{diag}(-1, 1, 1, 1)$, the equation of motion for the string world sheet $X^\mu(\sigma^a)$ is

$$\partial_a(\sqrt{-\gamma}\gamma^{ab}X^{\mu}_{,b}) = 0. \tag{A1}$$

Using the conformal gauge and $\sigma^0 \equiv \tau$, $\sigma^1 \equiv \sigma$ one obtains

$$\ddot{X}^{\mu} - X''^{\mu} = 0, \tag{A2}$$

and the gauge conditions are

$$\dot{\mathbf{X}} \cdot \mathbf{X}' = 0, \tag{A3}$$

$$\dot{\mathbf{X}}^2 + \mathbf{X}'^2 = 1. \tag{A4}$$

In this gauge, the world sheet coordinate τ can be identified with the Minkowski time coordinate t. The solution for (A2) can be written in terms of the right moving and the left moving waves as

$$\mathbf{X}(\sigma, \tau) = \frac{1}{2}[\mathbf{X}_+(\sigma_+) + \mathbf{X}_-(\sigma_-)], \tag{A5}$$

where the light cone coordinates are defined as $\sigma_+ \equiv \sigma + \tau$, $\sigma_- \equiv \sigma - \tau$. The corresponding gauge conditions are $\mathbf{X}'^2_+ = \mathbf{X}'^2_- = 1$, where primes denote derivatives with respect to the light cone coordinates.

Using the light cone coordinates, Eq. (5) can be written in the form

$$T(\mathbf{k}, \omega_n) = -\frac{\mu}{L}\int_{-L}^{L} d\sigma_+ \int_{-L}^{L} d\sigma_-(1 + \mathbf{X}'_+ \cdot \mathbf{X}'_-) \times e^{i/2[(\omega_n\sigma_+ - \mathbf{k}\cdot\mathbf{X}_+) - (\omega_n\sigma_- + \mathbf{k}\cdot\mathbf{X}_-)]}. \tag{A6}$$

Since we shall be mainly interested in modulus bursts from cusps, we use the expansion of the string world sheet about a cusp, which we take to be at $\sigma_+ = \sigma_- = 0$. The functions in the integrand of (A6) can be calculated from the expansions as

$$1 + \mathbf{X}'_+ \cdot \mathbf{X}'_- \approx -\frac{4\pi^2 s}{L^2}\sigma_+\sigma_-, \tag{A7}$$

and

$$\mathbf{k} \cdot \mathbf{X}_{\pm} \approx k\left(\pm\sigma_{\pm} \mp \frac{2\pi^2}{3L^2}\sigma^3_{\pm}\right), \tag{A8}$$

where s is an $O(1)$ parameter which depends on the loop trajectory and $\mathbf{k}$ is assumed to be in the direction of the string velocity at the cusp.

Equation (A6) can now be separated into two integrals as

$$T(\mathbf{k}, \omega_n) = \frac{4\pi^2\mu s}{L^3} I_+ I_-, \tag{A9}$$

where

$$I_{\pm} = \int_{-L}^{L} d\sigma_{\pm}\sigma_{\pm} e^{\pm i[(\omega_n - k\sigma_{\pm}/2) + (\pi^2 k/3L^2)\sigma^3_{\pm}]}. \tag{A10}$$

After a change of variables, we obtain the integral

$$I_{\pm}(u) = \frac{L^2}{2\pi^2}\left(\frac{\omega_n}{k} - 1\right)\int_{-\infty}^{\infty} dx x e^{\pm i(3/2)u[x + (1/3)x^3]}, \tag{A11}$$

where

$$u \equiv \frac{Lk}{3\sqrt{2}\pi}\left(\frac{\omega_n}{k} - 1\right)^{3/2}, \tag{A12}$$

and we have approximated the upper and lower limits of integration as $\pm\infty$. The real part of the integral is zero since it is an odd function of x. The imaginary part can be expressed in terms of the modified Bessel function,

$$I_{\pm}(u) = \pm i\frac{L^2}{2\pi^2}\left(\frac{\omega_n}{k} - 1\right)\frac{2}{\sqrt{3}}K_{2/3}(u). \tag{A13}$$

Then, (A9) can be calculated as

$$T(\mathbf{k}, \omega_n) = \frac{4L\mu s}{3\pi^2}\left(\frac{\omega_n}{k} - 1\right)^2 K^2_{2/3}(u), \tag{A14}$$

and the power spectrum for the moduli radiation (4) from a cusp is

$$\frac{dP_n}{d\Omega} = \frac{8L^2\alpha^2 s^2 G\mu^2}{9\pi^5}\omega_n k\left(\frac{\omega_n}{k} - 1\right)^4 K^4_{2/3}(u). \tag{A15}$$

The asymptotic form of the power spectrum for $k \gg m$ and $\omega_n \approx k$, i.e., $u \ll 1$, is[3]

$$\frac{dP_n}{d\Omega} \approx \tilde{\Gamma}\alpha^2 s^2 G\mu^2 n^{-(2/3)}, \tag{A16}$$

where $\tilde{\Gamma} \sim 1$. This is the same as the power spectrum for gravitons, except that for gravitons there is no additional coupling constant α and the numerical coefficient is somewhat different.

The average rate of moduli radiation per solid angle is

$$\frac{d\dot{N}}{d\Omega} = \sum_n \frac{1}{\omega_n}\frac{dP_n}{d\Omega}. \tag{A17}$$

The sum over n can be converted into an integral over k by using the relation $\omega_n = \frac{4\pi n}{L} = \sqrt{k^2 + m^2}$:

$$\sum_n = \frac{L}{4\pi}\int \frac{k dk}{\sqrt{k^2 + m^2}}. \tag{A18}$$

Here we only consider the modulus bursts which have very large Lorentz factors; thus we keep the leading order term in the limit $k >> m$. In this limit, (A12) becomes $u \approx \frac{Lm^3}{12\pi k^2}$. By substituting (A15) into (A17), using (A18), and also by making a change of variable $u \equiv \frac{Lm^3}{12\pi k^2}$, we obtain

$$d\dot{N} \sim \frac{\alpha^2 s^2 G\mu^2}{m} K^4_{2/3}(u) u^2 du d\Omega. \tag{A19}$$

The function $K_{2/3}(u)$ dies out exponentially at $u \gtrsim 1$. Hence, the main contribution to the rate comes from the region $u \lesssim 1$ which corresponds to

[3]When $u \ll 1$, $K_\nu(u) \approx \frac{\Gamma(\nu)}{2}(\frac{2}{u})^\nu$.

$$k \gtrsim k_{\min} = k_c \sim \frac{1}{4} m\sqrt{mL}. \tag{A20}$$

For $k >> k_{\min}$, Eq. (A19) gives

$$d\dot{N} \sim \alpha^2 s^2 G\mu^2 L^{1/3} k^{-5/3} dk d\Omega. \tag{A21}$$

From (A21), the number of moduli emitted from a cusp in a single burst, into solid angle $d\Omega$, having momentum between $(k, k + dk)$ can be estimated as

$$dN \sim L d\dot{N} \sim \alpha^2 s^2 G\mu^2 L^{4/3} k^{-5/3} dk d\Omega. \tag{A22}$$

Here, we assumed one cusp event per oscillation period of a loop.

Moduli are emitted into a narrow opening angle around the direction of the string velocity $\mathbf{v}$ at the cusp. The spectral expansion (A21) has been calculated for moduli emitted in the direction of $\mathbf{v}$. For moduli emitted at a small angle ϑ relative to $\mathbf{v}$, Eq. (A21) still applies, but now the spectrum is cut off at $k_{\max} \sim 1/L\vartheta^3$. In other words, the opening angle for the emission of particles with momenta $\gtrsim k$ is

$$\vartheta_k \sim (kL)^{-1/3}. \tag{A23}$$

Integration over Ω in (A21) gives a factor $\sim \vartheta_k^2$,

$$d\dot{N} \sim \alpha^2 s^2 G\mu^2 L^{-1/3} k^{-7/3} dk. \tag{A24}$$

The dominant contribution to the modulus emission comes from $k \sim k_{\min}$, and the total emission rate is

$$\dot{N} \sim \alpha^2 s^2 G\mu^2 L^{-1/3} k_{\min}^{-4/3}. \tag{A25}$$

The corresponding opening angle is

$$\vartheta_c \sim \gamma^{-1} \sim m/k_{\min}. \tag{A26}$$

The total power of the modulus radiation can be similarly calculated as

$$P \sim \alpha^2 s^2 G\mu^2 L^{-1/3} k_{\min}^{-1/3}. \tag{A27}$$

[1] A. Vilenkin and E. P. S. Shellard, *Cosmic Strings and Other Topological Defects* (Cambridge University Press, Cambridge, England, 1994).
[2] E. J. Copeland and T. W. B. Kibble, Proc. R. Soc. A **466**, 623 (2010).
[3] E. Witten, Nucl. Phys. **B249**, 557 (1985).
[4] V. Bereinsky, K. D. Olum, E. Sabancilar, and A. Vilenkin, Phys. Rev. D **80**, 023014 (2009).
[5] A. Babul, B. Paczynski, and D. N. Spergel, Astrophys. J. **316**, L49 (1987).
[6] V. Berezinsky, B. Hnatyk, and A. Vilenkin, Phys. Rev. D **64**, 043004 (2001).
[7] K. S. Cheng, Y. W. Yu, and T. Harko, Phys. Rev. Lett. **104**, 241102 (2010).
[8] T. Vachaspati, Phys. Rev. D **81**, 043531 (2010).
[9] T. Damour and A. Vilenkin, Phys. Rev. Lett. **78**, 2288 (1997).
[10] M. Peloso and L. Sorbo, Nucl. Phys. **B649**, 88 (2003).
[11] E. Babichev and M. Kachelriess, Phys. Lett. B **614**, 1 (2005).
[12] E. Sabancilar, Phys. Rev. D **81**, 123502 (2010).
[13] J. P. Conlon, F. Quevedo, and Kerim Suruliz, J. High Energy Phys. 08 (2005) 007.
[14] J. P. Conlon and F. Quevedo, J. Cosmol. Astropart. Phys. 08 (2007) 019.
[15] A. R. Frey and A. Maharana, J. High Energy Phys. 08 (2006) 021.
[16] C. P. Burgess *et al.*, J. High Energy Phys. 04 (2008) 053.
[17] W. D. Goldberger and M. B. Wise, Phys. Lett. B **475**, 275 (2000).
[18] F. Brummer, A. Hebecker, and E. Trincherini, Nucl. Phys. **B738**, 283 (2006).
[19] V. Berezinsky, P. Blasi, and A. Vilenkin, Phys. Rev. D **58**, 103515 (1998).
[20] R. Brandenberger, Nucl. Phys. **B293**, 812 (1987).
[21] V. Berezinsky and A. Vilenkin, Phys. Rev. Lett. **79**, 5202 (1997).
[22] V. Berezinsky and A. Vilenkin, Phys. Rev. D **62**, 083512 (2000).
[23] V. S. Berezinsky, Nucl. Phys. **B380**, 478 (1992).
[24] V. Berezinsky and M. Kachelriess, Phys. Rev. D **63**, 034007 (2001); S. Sarkar and R. Toldra, Nucl. Phys. **B621**, 495 (2002); R. Aloisio, V. Berezinsky, and M. Kachelriess, Phys. Rev. D **69**, 094023 (2004); C. Barbot and M. Drees, Phys. Lett. B **533**, 107 (2002).
[25] D. P. Bennett and F. R. Bouchet, Phys. Rev. D **41**, 2408 (1990).
[26] B. Allen and E. P. S. Shellard, Phys. Rev. Lett. **64**, 119 (1990).
[27] G. R. Vincent, M. Hindmarsh, and M. Sakellariadou, Phys. Rev. D **56**, 637 (1997).
[28] C. J. A. P. Martins and E. P. S. Shellard, Phys. Rev. D **73**, 043515 (2006).
[29] C. Ringeval, M. Sakellariadou, and F. Bouchet, J. Cosmol. Astropart. Phys. 02 (2007) 023.
[30] V. Vanchurin, K. D. Olum, and A. Vilenkin, Phys. Rev. D **74**, 063527 (2006).
[31] K. D. Olum and V. Vanchurin, Phys. Rev. D **75**, 063521 (2007).
[32] J. J. Blanco-Pillado, K. D. Olum, and B. Shlaer, Phys. Rev. D **83**, 083514 (2011).
[33] J. Polchinski and J. V. Rocha, Phys. Rev. D **75**, 123503 (2007).
[34] F. Dubath, J. Polchinski, and J. V. Rocha, Phys. Rev. D **77**, 123528 (2008).

[35] T. Damour and A. Vilenkin, Phys. Rev. D **71**, 063510 (2005).
[36] M. Sakellariadou, J. Cosmol. Astropart. Phys. 04 (2005) 003.
[37] M. G. Jackson, N. T. Jones, and J. Polchinski, J. High Energy Phys. 10 (2005) 013.
[38] V. Berezinsky and A. Smirnov, Astrophys. Space Sci. **32**, 461 (1975); V. Berezinsky, Nucl. Phys. **B380**, 478 (1992). For recent works see D. Semikoz and G. Sigl, J. Cosmol. Astropart. Phys. 04 (2004) 003; Z. Fodor, S. Katz, A. Ringwald, and H. Tu, J. Cosmol. Astropart. Phys. 11 (2003) 015; K. Kotera, D. Allard, and A. V. Olinto, J. Cosmol. Astropart. Phys. 10 (2010) 013.
[39] A. A. Abdo *et al.* (Fermi Collaboration), Phys. Rev. Lett. **104**, 101101 (2010).
[40] V. Berezinsky, A. Gazizov, M. Kachelrieß, and S. Ostapchenko, Phys. Lett. B **695**, 13 (2011).
[41] M. Ahlers *et al.*, Astropart. Phys. **34**, 106 (2010).
[42] N. Inoue *et al.* (JEM-EUSO Collaboration), Nucl. Phys. B, Proc. Suppl. **196**, 135 (2009).
[43] P. W. Gorham *et al.* (ANITA Collaboration), Astropart. Phys. **32**, 10 (2009); ()Phys. Rev. D **82**, 022004 (2010); Phys. Rev. Lett. **103**, 051103 (2009).
[44] A. Haungs, Nucl. Instrum. Methods A **604**, S236 (2009).
[45] O. Sholten *et al.*, Astropart. Phys. **26**, 219 (2006).
[46] C. W. James and R. J. Protheroe, Astropart. Phys. **30**, 318 (2009); R. D. Ekers *et al.*, Nucl. Instrum. Methods A **604**, S106 (2009).
[47] G. A. Gusev *et al.*, Nucl. Instrum. Methods A **604**, S124 (2009); V. A. Ryabov *et al.*, Nucl. Phys. B, Proc. Suppl. **196**, 458 (2009).
[48] G. Askarian, Sov. Phys. JETP **14**, 441 (1962).
[49] I. Kravchenko *et al.* (RICE Collaboration), Phys. Rev. D **73**, 082002 (2006).
[50] J. L. Christiansen *et al.*, Phys. Rev. D **83**, 122004 (2011).
[51] R. van Haasteren *et al.*, arXiv:1103.0576.
[52] S. Olmez, V. Mandic, and X. Siemens, Phys. Rev. D **81**, 104028 (2010).